Valles Marineris tectonic and volcanic history inferred from dikes in eastern Coprates Chasma

C. Brustel, Jessica Flahaut, E. Hauber, F. Fueten, Cécile Quantin, R. Stesky, R. Davies

AGU PUBLICATIONS

JGR

Journal of Geophysical Research: Planets

RESEARCH ARTICLE
10.1002/2016JE005231

Key Points:
- Dikes have different orientations on both side of the approximate location of the Coprates rise which coincide with a probable dichotomy
- Dike orientations record two distinct main tectonic stress fields (90° and 70°) and are different from the eastern part of Coprates Chasma

Supporting Information:
- Supporting Information S1
- Table S1

Correspondence to:
C. Brustel,
c.p.a.brustel@vu.nl

Citation:
Brustel, C., J. Flahaut, E. Hauber, F. Fueten, C. Quantin, R. Stesky, and G. R. Davies (2017), Valles Marineris tectonic and volcanic history inferred from dikes in eastern Coprates Chasma, *J. Geophys. Res. Planets*, *122*, 1353–1371, doi:10.1002/2016JE005231.

Received 28 NOV 2016
Accepted 30 APR 2017
Accepted article online 8 MAY 2017
Published online 22 JUN 2017

Valles Marineris tectonic and volcanic history inferred from dikes in eastern Coprates Chasma

C. Brustel[1,2], J. Flahaut[3], E. Hauber[4], F. Fueten[5], C. Quantin[2], R. Stesky[6], and G. R. Davies[1]

[1]Earth Sciences Department, Vrije University Amsterdam, Amsterdam, Netherlands, [2]Laboratoire de Géologie de Lyon: Terre, Planètes, Environnement, University of Lyon, Villeurbanne Cedex, France, [3]Institut de Recherche en Astrophysique et Planétologie, Université Paul Sabatier, Toulouse, France, [4]Institute of Planetary Research, German Aerospace Center, Berlin, Germany, [5]Department of Earth Sciences, Brock University, St. Catharines, Ontario, Canada, [6]Pangaea Scientific, Brockville, Ontario, Canada

Abstract Magmatic dikes have been proposed to have weakened and fractured the crust, allowing the formation of Valles Marineris. Hence, dikes were studied in the region of eastern Coprates Chasma in an area that includes a major transition between Hesperian-aged volcanic deposits in the western walls and pristine Noachian crust in the eastern walls. Over a hundred dikes were identified. Dike widths are 13 m on average. Estimation of magma eruption rates are comparable with previous estimates for Hesperian lava flows on Mars (10^5 to 10^6 m^3 s^{-1}). Dikes dips range from 55° to 90°; orientations record two distinct main tectonic stress fields (90° and 70°) different from the Chasmata. Dikes striking 90° are only observed at elevations below 1500 m. Dikes striking 70° are observed at elevation below 0 m and are therefore considered older. However, linear features are also observed on the late Noachian/early Hesperian surrounding plateaus and could be related to the 70° dike group. In the western part of our study area, dikes (~10% of the total amount of dikes mapped) strike 110, subparallel to Valles Marineris, and suggest a relationship between dike emplacement and graben formation. The presence of preexisting faults in the two directions (90° and 70°) could explain the shape of eastern Valles Marineris and chaotic terrains, which have a different general orientation than the Valles Marineris main rift. Our results suggest a complex relationship between dike emplacement and the formation of Valles Marineris.

1. Introduction

The Tharsis bulge is a vast volcanic province that covers almost a quarter of the Martian surface and is elevated up to 10 km. The Tharsis bulge exhibits concentric compressional and radial extensional tectonic features such as graben systems, including the Valles Marineris canyon system [*Carr*, 1974; *Wise et al.*, 1979]. Valles Marineris is a 4000 km long, 300 km wide trough system near the Martian equator that is up to 11 km deep. This unique natural cut provides insights into the geologic evolution of the Martian crust, exposing rocks from the Noachian to the Amazonian eras. Since its discovery by Mariner 9 in 1971 [*Sharp*, 1973; *Carr*, 1974], the formation mechanism of Valles Marineris has remained a matter of debate. Although Tharsis tectonic and volcanic activity is estimated to have started in the early Noachian (4.1–3.95 Gyr), followed by crustal thickening during the mid-late Noachian (3.95 to 3.7 Gyr), [*Johnson and Phillips*, 2005], the formation of Valles Marineris was not completed until the late Hesperian (3.7–3.0 Gyr) [e.g., *Quantin et al.*, 2004] or Amazonian (<3.0 Gyr) [e.g., *Baker et al.*, 1992; *Lucchitta et al.*, 1994; *Fueten et al.*, 2011]. An intermediate stage may have involved the formation of closed ancestral basin prior to linking of the subtroughs that now form Valles Marineris [*Baker et al.*, 1992; *Lucchitta et al.*, 1994]. This hypothesis is supported by the irregular shape of some troughs (e.g., Melas, Ophir, and Capri Chasmata), their lower average elevation compared to the connecting troughs, and the presence of interior layered deposits on these trough floors. *Schultz* [1998] proposed that magmatic intrusions could have provided structural control for the development of the ancestral basin.

It is still debated, however, whether Valles Marineris was formed as the result of normal faulting, collapse, or in response to magmatic intrusions. Potential collapse mechanisms include the formation of Valles Marineris trough tension fractures [*Tanaka and Golombek*, 1989]. In this model, tension fractures propagated trough the crust resulting in grabens. The collapse of material in voids produced by tension fracture initiates the formation of pit chains. More extension, erosion, landslides and removal of the material, enlarged the pits,

and subsequent extension formed the trough. This implies enormous void volume, but the mechanism of material removal is as yet unexplained. Another hypothesis involving collapse is the action of thermokarst and karst-like processes. The thermokarst hypothesis assume that the Martian surface collapsed after ice removal in the upper surface [*Sharp*, 1973]. *Croft* [1989] proposed carbonate dissolution and subsequent collapse of cavities instead of ice removal as a mechanism to form Valles Marineris. These models imply large amounts of ice or carbonate in the lithosphere, for which there is currently no evidence. An alternative model is that Valles Marineris formation was controlled by dike emplacement radial to Syria Planum, a volcanic center of the Tharsis region, that occurred during late Noachian/early Hesperian [*Mège and Masson*, 1996]. Grabens formed radial to Syria Planum and were associated with lava flows and resurfacing. A later episode of diking with a second set of grabens, approximately centered on the actual Tharsis Montes ("Tharsis-centered"), was superimposed on the previous graben set. Dike emplacement was proposed to be the origin of crustal extension, graben formation, and large troughs formation such as Valles Marineris.

Rifting was also suggested based on the observations of 40° to 55° dipping normal faults [*Schultz and Lin*, 2001]. *Andrews-Hanna* [2012a], however, pointed out uncertainties in the model. The authors predicted that low to moderate dipping faults would have produced important deformation such as an uplift of the lithosphere in the surrounding plateaus, which is not observed. They concluded that only rift formation through subvertical faults, dipping at least 85°, was consistent with the actual topography [*Andrews-Hanna*, 2012a].

The presence of dikes in Valles Marineris was recently reported by *Flahaut et al.* [2011]. The orientation of three dikes is approximately east-west, roughly parallel to troughs, suggesting that magmatic intrusions could have directly led to the formation of Valles Marineris by cutting the crust and facilitating block subsidence [*Andrews-Hanna*, 2012c].

The present paper provides a detailed analysis of the dikes in the eastern part of Coprates Chasma, eastern Valles Marineris (Figure 1). In order to understand the role of dikes in the tectonic and volcanic histories of Valles Marineris and to fully characterize them, we used imagery and altimetry data from the CTX (ConText Camera) [*Malin et al.*, 2007], HiRISE (High Resolution Imaging Science Experiment) [*McEwen et al.*, 2007], and MOLA (Mars Orbiter Laser Altimeter) [*Smith et al.*, 2001] instruments. The overall distribution, orientations, elevations, and dips of over a hundred dikes exposed in the walls of the trough were measured. Dike dimensions were input into an eruption rate model in order to estimate potential eruption rates, which were compared with values previously estimated for fissure eruptions on Mars [e.g., *Head et al.*, 2006; *Hiesinger et al.*, 2007; *Hauber et al.*, 2011]. Mapping and modeling results are integrated to reconstruct part of the geologic history of the eastern part of Coprates Chasma and critically examine existing tectonic models.

2. Data and Methods

A geographic information system (GIS) was built using imagery data from various Martian orbiters. Thermal Emission Imaging System (THEMIS) daytime and nighttime data from the Mars Odyssey mission, which is available as two global mosaics of 100 m per pixel spatial resolution, were used as a background. Coprates Chasma walls have been extensively targeted by the Mars Reconnaissance Orbiter (MRO) mission instruments, and the region is fully imaged at Context Camera (CTX) scale. High-resolution data from the HiRISE and CTX were used for detailed mapping. CTX data were calibrated and projected using the U.S. Geological Survey projection-on-the-web tool [*Hare et al.*, 2013]. HiRISE images have a ground pixel size of 0.25 m, and their central swath provides three spectral channels that were used as false-color combinations to highlight compositional differences. CTX images (6 m per pixel) were used to track dikes and stratigraphic units along the walls where HiRISE images were lacking. MOLA data were used to determine elevations. Dimensions and elevations were measured using ArcGIS tools (Environmental Systems Research Institute), and azimuths were calculated with the PolarPlots extension for ArcGIS (Jennessent Entreprise). Dike widths were measured orthogonally to the length in the most exposed parts of the dike. Dike dips were measured with the software program Orion [*Fueten et al.*, 2008] where HiRISE digital terrain models (DTMs) or HiRISE stereo-pairs were calculated using the NASA Ames Stereopipeline [*Moratto et al.*, 2010; *Broxton and Edwards*, 2008]. Orthorectified images were also constructed when possible and used to measure dike dimensions and azimuths more precisely. All images shown in this study are projected with north to the top.

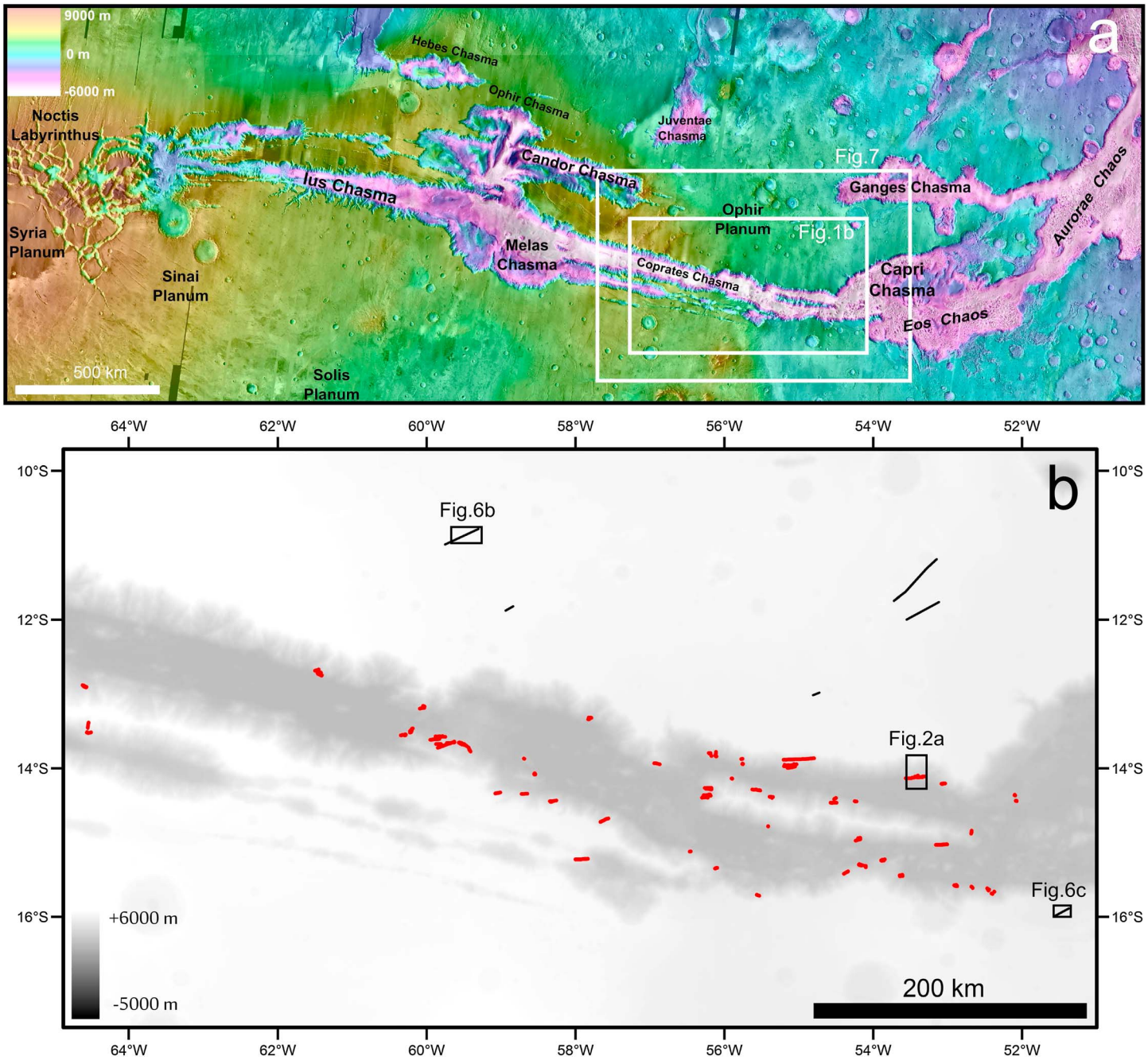

Figure 1. (a) Location of Coprates Chasma (white box) within the Valles Marineris region (background: colorized MOLA elevation map overlain on THEMIS IR daytime data). (b) Close-up of the study area centered in the eastern part of Coprates Chasma. The red lines represent features that were mapped as dikes in Coprates Chasma walls; the black lines represent possible dikes or other tectonic features on the surrounding plateaus (background: MOLA elevation map).

3. Regional Context

Coprates Chasma is a 1000 km long, 100 km wide, linear trough connecting Melas Chasma (central Valles Marineris) to Capri Chasma (eastern Valles Marineris). Our study area is located in eastern Coprates Chasma, between 11°S and 18°S in latitude and 51°W and 65°W in longitude (Figure 1). The north and south walls and central horst flanks of Coprates Chasma contain numerous continuous outcrops that can exceed 6 km in height. Four different stratigraphic units have been identified along the walls of eastern Coprates Chasma [see Figure 2 and *Flahaut et al.*, 2012]. (1) The topmost unit is composed of horizontal layers with no specific spectral signature, consistent with a stack of lavas. (2) Outcrops become sparser and layering less obvious in

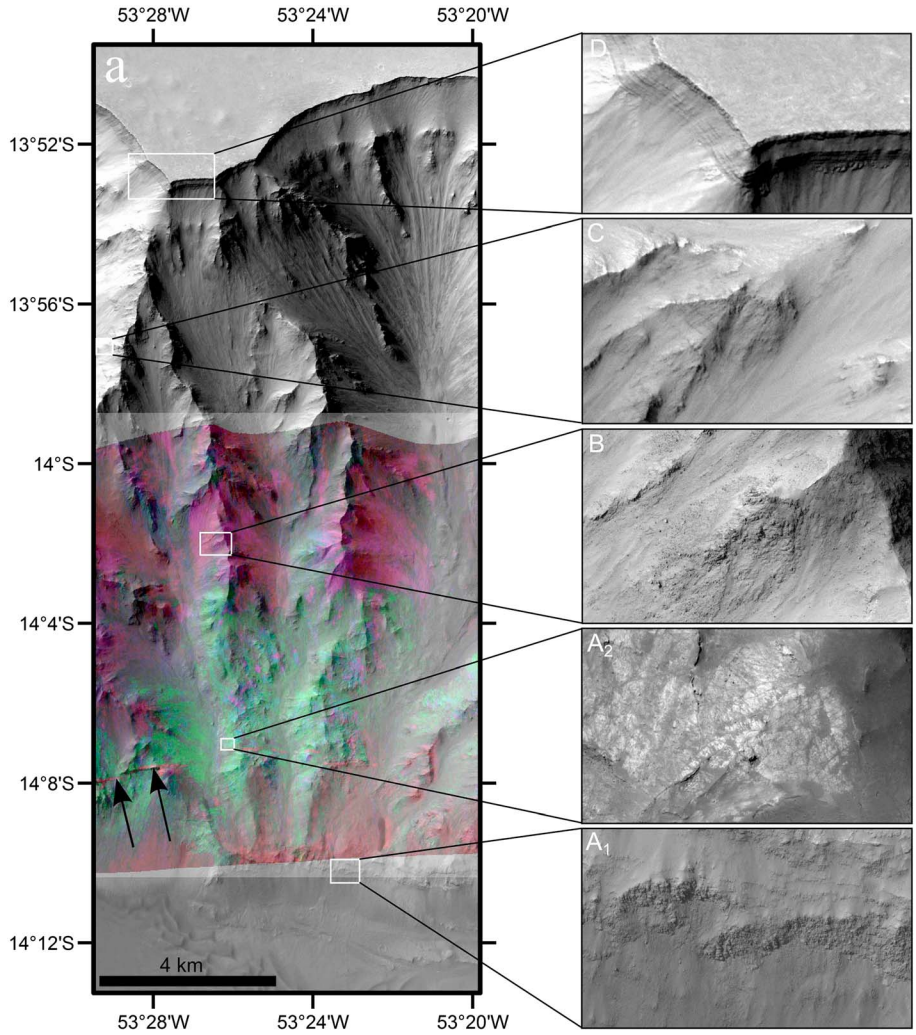

Figure 2. (a) CTX mosaic showing a portion Coprates Chasma northern wall from the floor (−4000 m) to the plateau (+2400 m). CRISM FRT00009DB4 RGB composite of summary parameters OLINDEX2, LCPINDEX2, and D2300 is overlain as a transparency over CTX images in the bottom walls (stretched values: R: 0.015–0.046, G: 0.009–0.039, and B: 0–0.024). Fe/Mg-rich phyllosilicate detections (wall unit B) are mapped in magenta, low calcium pyroxene detections in green (unit A2), and olivine detections in red (dike + unit A1). The black arrows point to the location of an olivine-rich dike. [modified after *Flahaut et al.*, 2011]. Close-up on the different units defined by *Flahaut et al.* [2012] is shown on the right (HiRISE psp_007218_1660 and CTX images). A = Pristine Noachian crust (A1: stratified, dark layers, A2: light-toned crust with meter to decameter-scale fractures) with a variable thickness of about 2000 m; B: phyllosilicate-rich layer 1500 m thick. The transition between the A and B layers is progressive; C: Talus slope 2500 m thick; D: topmost unit, stack of Hesperian and Noachian lava flows 500 m thick, with meter- to decameter-scale layering visible. See also Figure 5a.

the second unit located at middle elevations where the walls are dominated by talus and likely composed of less competent material or could be composed of material accumulated from the upper levels. (3) The third unit is composed of dark boulders, in which Fe/Mg-rich phyllosilicates are detected. This unit has a variable elevation and thickness (1500 m in average [see *Flahaut et al.*, 2012, Figure 7 and Table S1 in the supporting information]) along the walls but is always observed on the top of a massive bedrock (referred to a pristine crust) that forms the fourth and basal unit. The phyllosilicate-rich unit could have been formed by aqueous alteration of the pristine crust at its surface or could represent weathered lava flows that were emplaced after the crust formation, and altered in a wet environment [*Flahaut et al.*, 2012]. (4) The pristine, Noachian crust unit is made of light-toned, highly fractured rocks, characterized by orthopyroxene signatures. *Flahaut et al.* [2012] also reported that some portions are composed of darker, olivine-rich material with possible layers, making the basement locally heterogeneous. This light-toned, lower unit was previously interpreted as a potential remnant of primitive crustal outcrops [*Flahaut et al.*, 2012]. Vertical stratification generally applies to all

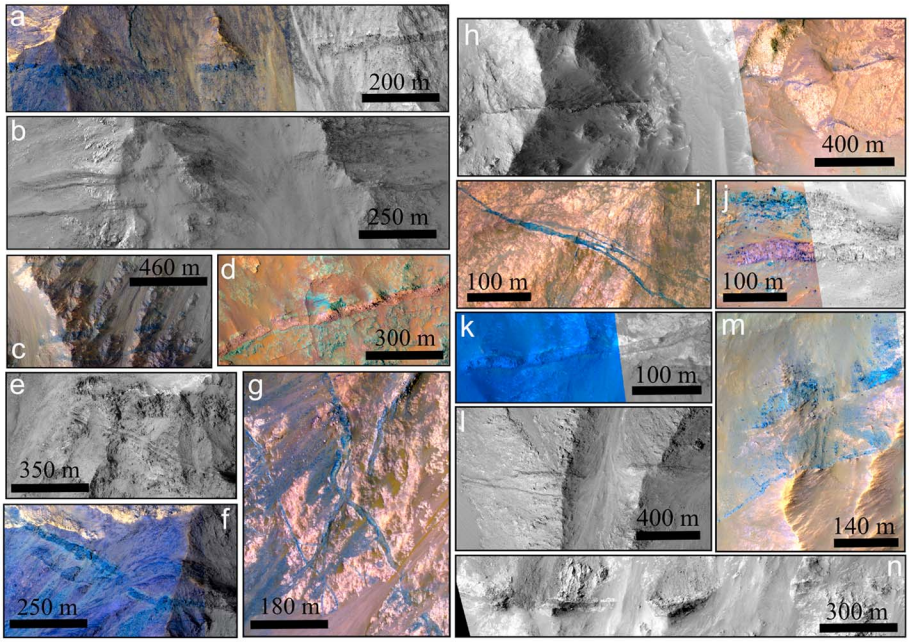

Figure 3. HiRISE views of dikes in Coprates Chasma walls. (a) HIRISE ESP_013191_1660 and (b) HIRISE PSP_010857_1650, east-west kilometer long dikes crosscutting the northern wall; (c) HIRISE ESP_039129_1655, dark-tone dike cluster in the southern wall; (d) HIRISE ESP_013903_1650, a dike crosscutting the central horst southern wall; (e) HIRISE PSP_004159_1660, a 110° dike crosscutting the northern wall; (f) HIRISE ESP_039353_1660 dike with light-toned bordure crosscutting the northern wall; (g) HIRISE ESP_03967_1670, small-scale dike or fracture cluster crosscutting the northern wall; (h) HIRISE PSP_003513_1665 + IRB, kilometer-long dike crosscutting the southern wall; (i) HIRISE ESP_040461_1670, small-scale dike or fracture in the light-toned crust; (j) HIRISE PSP_003513_1665, east-west dike (purple) with darker margin and possible horizontal columnar jointing; (k) HIRISE ESP_039063_1660 + IRB, dike with darker margin; (l) HIRISE ESP_013547_1655, dike cluster with positive relief due to differential erosion; (m) HIRISE ESP_025639_1660 + IRB, two parallel dikes in blue color crosscutting the southern wall; and (n) HIRISE ESP_027340_1645, possible east–west dark-tone dike with a distinct light margin.

chasmata of eastern Valles Marineris. By contrast, the walls of western Valles Marineris appear to be formed of different material, likely volcanic in nature, which indicates the presence of a major discontinuity (large-scale tectonic, volcanic, or impact structure) in western Coprates Chasma [*Flahaut et al.*, 2012; *Quantin et al.*, 2012]. Our study area straddles the transition zone between the two distinct lithologies observed in eastern and western Valles Marineris.

The three dikes previously reported in eastern Coprates Chasma intrude the massive light-toned crust at the base of the chasma walls [*Flahaut et al.*, 2011]. These dikes are made of a dark material and form a marked contrast with the light-toned crust unit of Valles Marineris eastern walls. Although the light-toned, massive, fractured crust also outcrops in the lower parts of nearby chasmata (Capri, Gangis, Juventae, and western Coprates), exposures are more extensive in eastern Coprates Chasma. Indeed, contrary to most Valles Marineris chasmata, Coprates Chasma contains little to no interior layered deposits [e.g., *Fueten et al.* [2011]] and is affected by few landslides [*Quantin et al.*, 2004]. Walls in eastern Coprates Chasma are therefore well exposed and preserved and have been targeted by the MRO instruments. Dikes have not previously been identified in the western part of Coprates Chasma. Outcrops in this region are less well exposed and made of a different, less competent material, often covered by dusty talus making dike detection more difficult.

4. Identification and Characterization of the Dikes

4.1. Mapping and Distribution

Over a hundred linear features interpreted as dikes were discovered, mostly in the eastern part of Coprates Chasma (Figures 1b and 3). Exposed dikes are narrow, generally linear features but locally slightly arcuate where there are significant topography changes. Dikes crosscut topographic highs and stratigraphic layers in the walls of Valles Marineris. Dikes often appear in relief and hence are relatively resistant to erosion

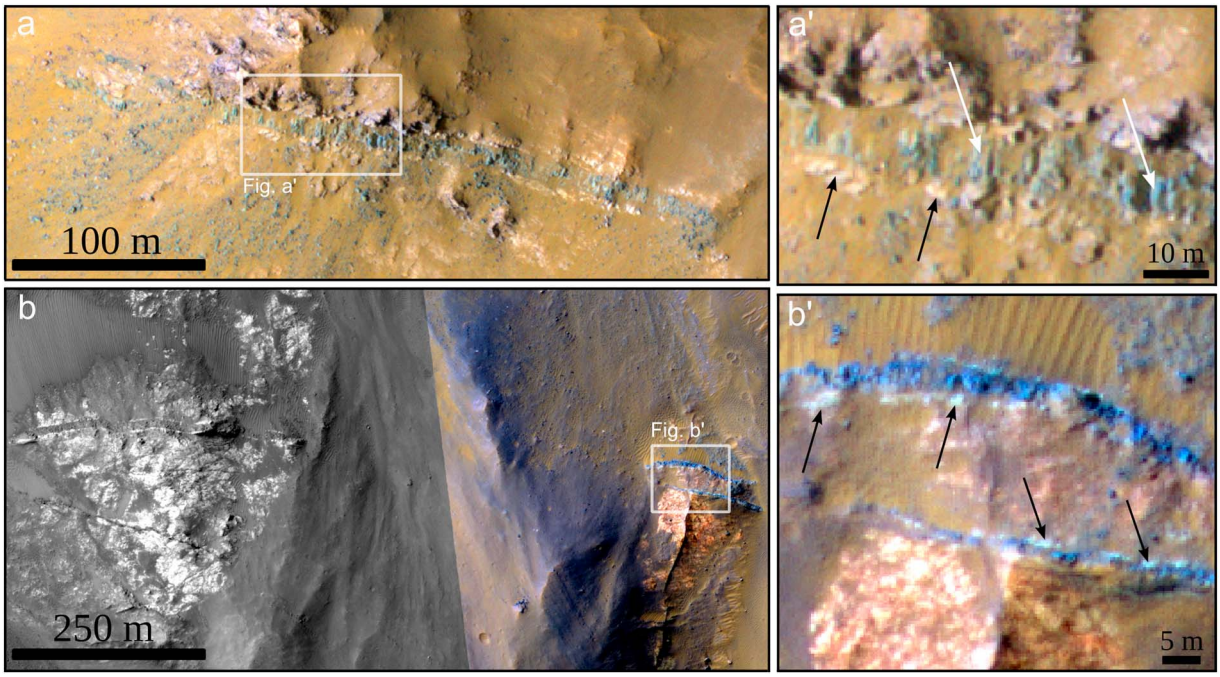

Figure 4. Close-up on dikes with metamorphic borders and possible columnar jointing. (a) HiRISE ESP_020773_1655 false-color (IRB) showing a dike located at the junction between Coprates and Capri Chasmata. The dike appears bluer than the metamorphic border which appears white on the color composite (black arrows). The white arrows point at possible columnar jointing. (b) Composite image, HiRISE ESP_034856_1655 RED + false color (IRB), showing several dikes in the central horst of Coprates Chasma. The fractured light-toned crust is well exposed on the left showing an east-west dike with smaller dikes or fractures. On the right, the same dike and another smaller one. They appear blue (IRB composition) with a white metamorphic border (black arrows). (a′ and b′) Close-ups on the dike sections of Figures 4a and 4b.

and do not appear to be internally stratified. Dikes cannot always be identified with CTX images alone and are most easily identified on the HiRISE panchromatic and color images. Their width remains broadly constant over their observable length. Using HiRISE false-color images, dikes can be distinguished from the host rock as they are made of a spectrally distinct material, especially when they are located in the lower part of the walls, in the light-toned crust. Distinct margins outline the largest dikes and are interpreted as zones of contact metamorphism (Figure 4b). These margins appear lighter-toned than the dike and sometimes the host rock. Factures within the dikes perpendicular to the dike margin are sometimes visible and are interpreted as columnar jointing due to magma cooling (Figure 4a).

Dikes are ubiquitous in the study area being observed in the north and south walls of Coprates Chasma and the walls of its central horst. Eighty percent of the dikes are observed in the light-toned pristine Noachian crust at lower elevations of the chasma walls between −3500 m and −2500 m (Figure 5a). Dikes are also found at higher elevations, intruding more recent layers composed of lava flows. The difference in the number of dike detections at different elevation may be related to variation of volcanic activity during the Noachian. Alternatively, dike detection may be more difficult to detect by color contrast in the upper dark layers. The presence of dikes on the surrounding plateaus is more difficult to confirm with certainty due to the lack of HiRISE imagery. Possible dikes on the plateau appear as long (5 to 50 km) and thin (20 to 50 m) linear ridges probably exposed due to differential erosion. These linear features could potentially be other geological features such as faults related to the same tectonic event. Eighteen dikes are also observed and mapped in the western part of Coprates Chasma; however, the poorer quality of wall outcrops, which are of a different nature than the eastern walls [*Flahaut et al.*, 2012], makes the identification and quantification of the dikes more difficult. Metamorphic borders and columnar jointing, unequivocal criteria used to identify a dike, are not always observed, and some of these features could also correspond to fractures or faults.

4.2. Dike Dimensions

Dike lengths and widths were measured on HiRISE imagery, using well-exposed sections only. The average width value of one dike cannot be well constrained as only small-scaled segments are observed. When

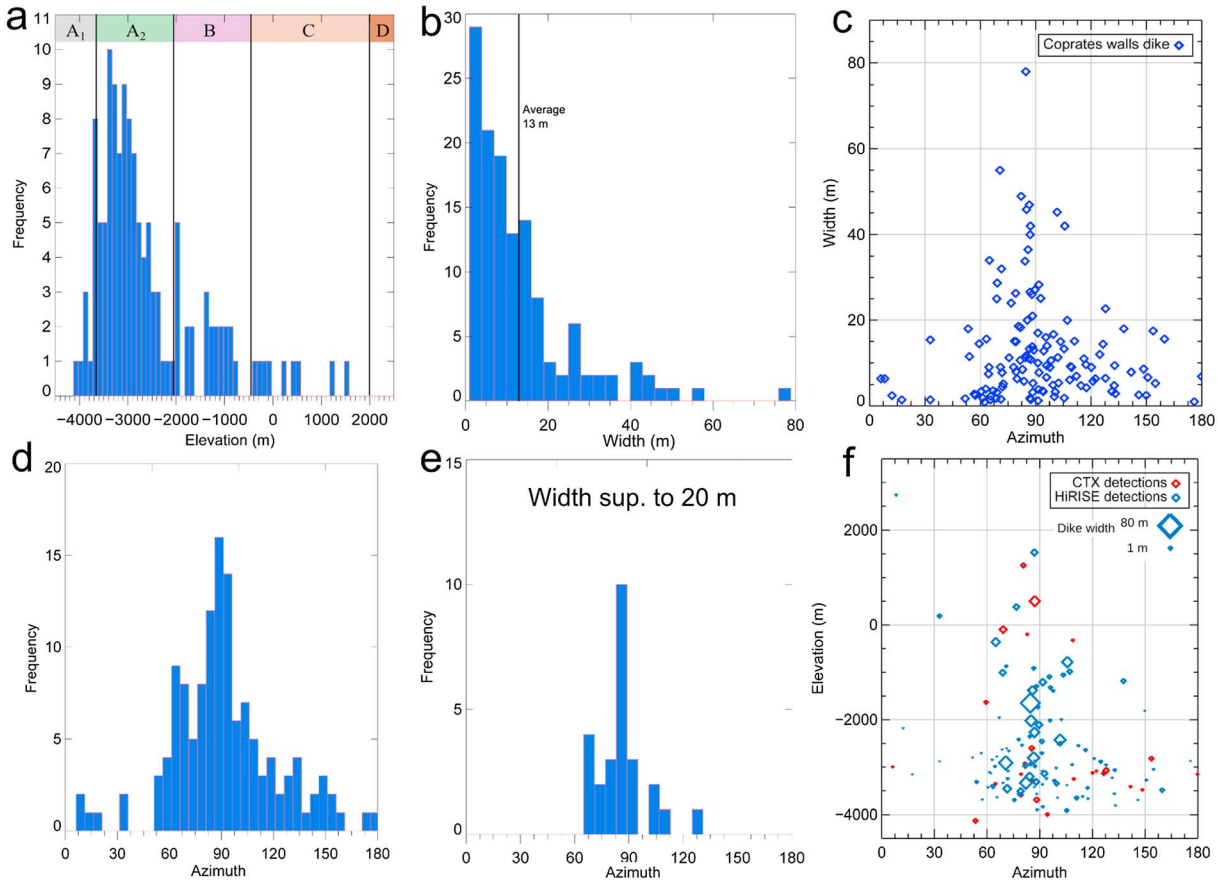

Figure 5. Characteristics of the dikes mapped in the walls of Coprates Chasma. (a) Histogram of dike altitude in eastern Coprates Chasma (the altitude corresponds to the maximum altitude observed for each dike). Boundaries of the horizontal units defined by *Flahaut et al.* [2012] are reported (from bottom to top): A = fractured Noachian crust (A_1: stratified, darked layers, A_2: light-toned fractured blocks), B: phyllosilicate-rich layer, C: Talus slope, and D: top-most unit, stack of Hesperian and Noachian lava flows with layered visible. Dike density is higher in the light-toned fractured blocks where dikes are more easily detected. (b) Histogram frequency of dikes width in Coprates Chasma walls. The average width is 13 m; smaller dikes (width ~ 1 m) are most commonly observed. (c) Dike widths as a function of dike azimuths. Smaller dikes are oriented in all directions whereas the wider dikes have orientations ranging between 60° and 100°. Due to the irregularity of the dike widths along their length, and the impossibility to observe the entire dike, the uncertainty on this value can be up to 30% in the case of a subvertical dike (see text). (d) Histogram of dike azimuth. The most common azimuth occurs at ~90°, but there is a second maximum at ~70°. Very few dikes have strikes below 60°or above 160°. (e) Histogram of azimuth for dikes wider than 20 m, which again show two maxima at 70° and 90°. (f) Dike elevations as a function of their azimuths. The size of the diamond symbol represents dike widths. The smaller dikes are mostly observed at elevation ranging from the canyon floor to −2000 m and show various azimuths. The widest dikes are found throughout the chasma walls with azimuths between 60° and 100°.

possible, dike widths were measured at several locations along the same dike and an average was taken. We observed that dike widths have a variability <30% along the dike length (Figures 3b and 3i). Measured dike widths range from small-scale intrusions, hardly detectable with HiRISE (<1 m) to intrusions up to 78 m in width. The average dike width in the study area is 13 m (Figure 5b), but this value is likely biased as smaller dikes can only be identified where HiRISE observations are available (Figure 5a). Dike lengths are difficult to estimate as dikes are partially covered by talus and HiRISE data coverage is sparse. In some cases, several parts of the same, few kilometer-long dike can be tracked along a wall spanning several HiRISE or even CTX images for the longest dikes, making it possible to estimate minimum lengths. The longest dike can be followed for a distance of 20 km. No significant changes were observed in the dike dimensions as measured on nonrectified and orthorectified images (when available).

4.3. Dike Azimuths and Dips

Dikes are oriented between 0° and 180° (Figure 5c) with a greater range of azimuths observed for thinner dikes (<20 m in width) that could include fractures or faults, with scattered orientations controlled by local host rock characteristics. Considering only wider dikes (> 20 m), less variation in orientations are recorded and two main orientations are defined: 90° and 70° (Figure 5e). There is a noticeable difference in elevation ranges over

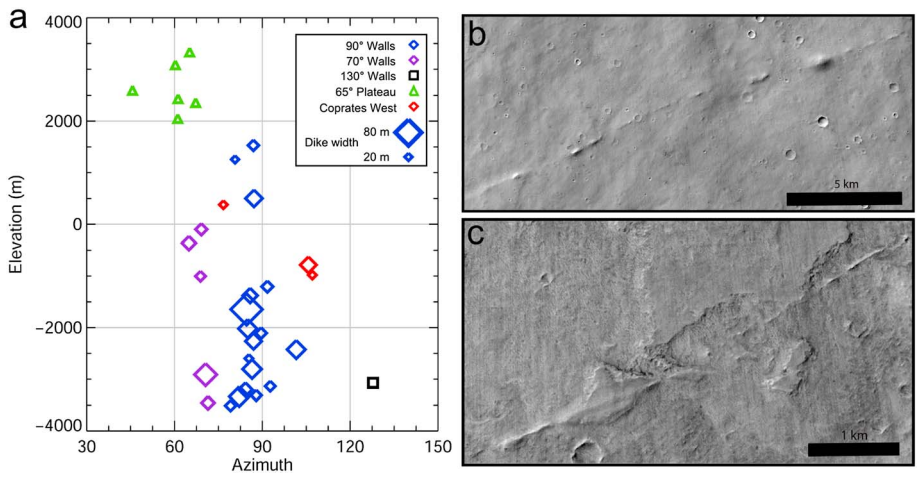

Figure 6. Putative dikes observed on the surrounding plateaus. (a) Dike altitudes as a function of their azimuths. Only dikes with widths larger than 20 m are represented. Symbol size represent the dike widths. The blue, purple, and black squares are dikes in the eastern part of Coprates Chasma. The green triangles represent putative dikes on the plateau mostly oriented 65°. The red squares are dikes in the western part of Coprates Chasma. Two dike groups are visible with orientations of ~70° (red squares) and ~90° (blue squares). (b and c) CTX images showing putative dikes on the plateau, which are oriented ~70°: CTX P09_004594_1653_XN_14S051W and CTX B19_016857_1693_XN_10S059W, respectively.

which dikes of different orientations were observed. Dikes striking 90° are observed at elevations below 1500 m in the walls, whereas dikes striking 70° are observed until 0 m. Possible 70°-striking dikes on the plateau (Figure 6) indicate that they may crosscut the entire wall height even though they are yet to be detected in the uppermost levels of the chasma walls. Dikes in the western part of Coprates Chasma seem to have different orientation with a majority oriented between 110° and 140° (Figure 7). No crosscutting dike relationships were observed during this study. The geometry of Valles Marineris outcrops may introduce a detection bias. Indeed, dikes perpendicular to the wall would be favored and dikes striking parallel to the walls would be less observed. However, due to the gentle slope of the walls (30°) this bias would not be significant.

Dike dips were measured where possible using HiRISE DTMs. The difference in azimuth between projected and orthorectified HiRISE images was less than 5°. Fifteen measurements were made on dikes located in the north and south walls and the central horst on Eastern Coprates Chasma. Dips range from 55 to 90° with an average of 72°, suggesting that dikes are near vertical features. Furthermore, even when DTM are missing, dikes crosscutting spurs are straight features which also indicates that they are subvertical as seen in Figures 3a, 3b, 3h, and 3i; with exceptions in Figures 3g and 3f and 4b which show curved dikes having probable significant dips. Differences in dips do not appear to correlated to dike location (e.g., north or south walls). Within the same wall, some dikes dip both north and south, which suggests that they do not use (only) existing trough-forming normal faults.

5. Modeling of Dikes Eruption Rates

The upper part of Coprates Chasma is composed of stack of lava flows of undetermined origin [e.g., *Mcewen et al.*, 1999]. We assume that dikes could have fed these lava flows. To evaluate this possibility, the hypothetical amount of magma erupted by the dikes was determined using the equations of *Wilson et al.* [2009] based on the dike dimensions and assumed magma properties. The time required to form the topmost basaltic layers was also estimated.

Equations (1a) and (1b) give the magma flow speed:

$$u = \left(W^2 dP/dz\right)/(12\eta) \quad \text{for a laminar flow motion} \tag{1a}$$

$$u = \left[(WdP/dz)/(f\rho)\right]^{1/2} \quad \text{for a turbulent flow motion} \tag{1b}$$

where W is the measured dike width, dP/dz is the pressure gradient driving magma motion, η is the magma viscosity, ρ is the magma density, and f is the friction coefficient [*Wilson et al.*, 2009]. Dike widths were

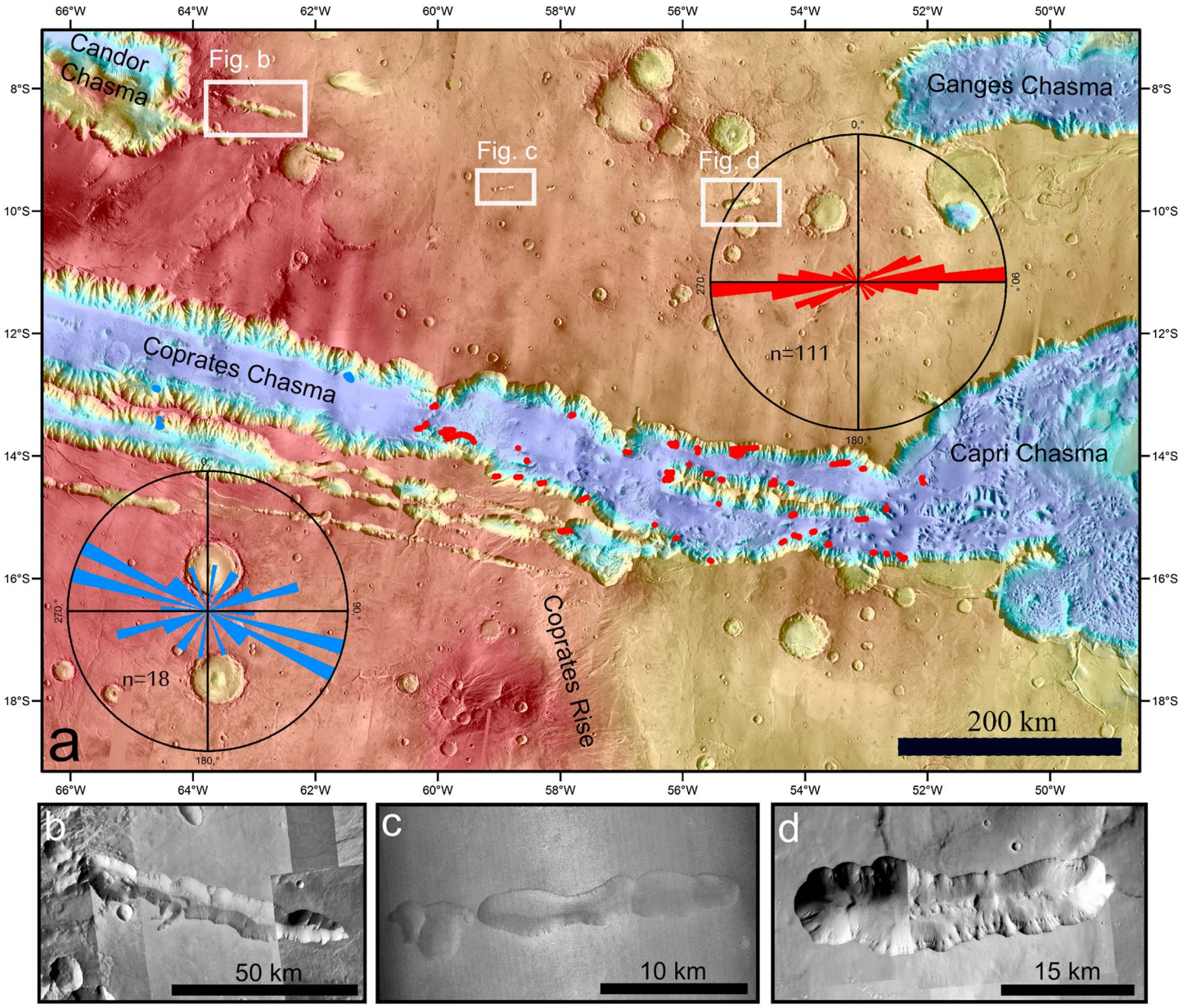

Figure 7. (a) Dike orientations in the Coprates Chasma region (background: Colorized MOLA elevation map overlain on THEMIS IR daytime data). The rose diagrams show dike orientations in eastern (red) and western (blue) Coprates Chasma. The red lines are mapped dikes in the eastern part of Coprates Chasma and are mostly oriented 90°. The blue lines show the location of dikes in the western part of Coprates Chasma, which appear oriented between 95° and 130°. (b) Close-ups of pit chains and pit troughs to the north of Coprates Chasma which are striking ~110° in the west. (c and d) Pit chains and pit troughs striking ~90° in the east. Locations are indicated in CTX B02_010620_1719_XN_08S063W, P07_003645_1729_XI_07S063W, P11_005346_1735_XI_06S063W, P12_005557_1736_XI_06S063W, and B22_018057_1710_XN_09S062W (Figures 7a and 7b); CTX P09_004647_1684_XN_11S058W (Figure 7c); and CTX P20_009011_1703_XN_09S055W and B06_011991_1703_XN_09S055W (Figure 7d).

measured at several places along the observable length of each dike to compute an approximate mean value. Total dike lengths are poorly constrained as they are always partially buried (<20 km). Length estimates are therefore necessarily a minimum estimate, especially when dikes only appear as meter-long segments and represent a major source of uncertainty in the calculations.

The dike lengths were estimated using empirical values of aspect ratios reported in the literature. These ratios range between 10^2 and 10^4 [*Rubin*, 1995]. Similarly, aspect ratios for 12 basaltic dikes located in Iceland range between 0.3×10^3 and 1.5×10^3 [*Gudmundsson*, 1984]. The aspect ratio for Martian dikes is poorly constrained; therefore, a value of 10^3 was chosen for the calculation. Even with the use of an aspect ratio

of 10^3, dike lengths could still be underestimated (where terrestrial dikes were measured with aspect ratios >3000 [e.g., *Ernst and Bell*, 1992; *Baragar et al.*, 1996]), but the assumed lengths are greater than what can be measured on current observations, suggesting that actual eruption rates are higher than the ones estimated from measured lengths.

Based on the existing literature, dP/dz was set to 500 Pa m^{-1} as a minimum pressure gradient needed to raise the magma to the surface of Mars and cause an eruption [see *Wilson et al.*, 2009]. The magma viscosity, η, could not be measured directly. Estimates from previous studies of lava flows morphology range from 10^2 to 10^8 Pa s [*Zimbelman*, 1985; *Wilson et al.*, 2009; *Hauber et al.*, 2011]. A recent experimental study [*Chevrel*, 2013] suggests lower viscosities (<1 Pa s) at liquidus conditions for studied synthetic silicate liquids representative of the diversity of Martian volcanic rocks including primary Martian mantle melts and alkali basalts. A lower viscosity would result in higher eruption rates.

Values 10, 100, and 1000 Pa s were chosen to cover a range of viscosities corresponding to fissural, presumably basaltic, eruptions previously studied in the Tharsis region [*Hiesinger et al.*, 2007; *Wilson et al.*, 2009; *Hauber et al.*, 2011].

The magma density, ρ, was set at 2500 kg m^{-3} as assumed by *Wilson et al.* [2009] in the Tharsis region. Although earlier studies suggested higher values (2500 to 2900 kg m^{-3} [*Moore et al.*, 1978], 2750–2960 kg m^{-3} [*Longhi*, 1990], and 2600 kg m^{-3} [*Cattermole*, 1987]), more recent studies used a similar value of 2500 kg m^{-3} to allow some vesicularity in the lava [e.g., *Wilson et al.*, 2009] (see *Hiesinger et al.* [2007] for a complete review).

The friction coefficient f was set to 0.01, which corresponds to the friction of a dike-like conduit according to previous literature [*Wilson and Head*, 1981; *Wilson and Head*, 2001].

The Reynolds number can be calculated to determine if magma flow in a dike is turbulent or laminar:

$$\mathrm{Re} = (2uW\rho)/\eta \tag{2}$$

The magma ascent speed, u, is needed to calculate the Reynolds number. A method proposed by *Wilson et al.* [2009] is to first assume a laminar flow regime, then calculate the magma ascent speed for that case, and finally calculate the associated Reynolds number. If the result is much greater than the critical value for turbulent flow (~2000), then the regime flow is likely to be turbulent and the Reynolds number calculated using the result of equation (1b) will also correspond to a turbulent flow.

The magma ascent speed was calculated for each dike. The eruption rate per meter of length, F ($m^3\ s^{-1}\ m^{-1}$) is given by equation (3):

$$F = uW \tag{3}$$

Then, the total lava volume flux E ($m^3\ s^{-1}$) of each dike is given by

$$E = FL \tag{4}$$

where L is the dike's length (measured or derived from the empirical aspect ratio). Table S1 in the supporting information shows the values of E calculated for each dike.

Assuming a magma viscosity of 10 Pa s, all dikes are in a turbulent flow regime. Eruption rates range from 3 $m^3\ s^{-1}\ m^{-1}$ for 1 m wide dikes to 3×10^3 $m^3\ s^{-1}\ m^{-1}$ for the widest dike (~78 m) with an average of 291 $m^3\ s^{-1}\ m^{-1}$. Using the measured lengths in eastern Coprates Chasma (likely a major underestimate), eruption rates for individual dike range from 1.3×10^3 to 2.3×10^7 $m^3\ s^{-1}$ with an average of 1.6×10^6 $m^3\ s^{-1}$. Using the empirically estimated dike lengths, eruption rates range from 2.7×10^3 to 2.4×10^8 $m^3\ s^{-1}$.

Assuming a magma viscosity of 100 Pa s, the dike regime transitions from laminar to turbulent at a width of ~4.5 m. Eruption rates range from 0.3 to 3×10^3 $m^3\ s^{-1}\ m^{-1}$ with an average of 289 $m^3\ s^{-1}\ m^{-1}$. Using the measured dike lengths in eastern Coprates Chasma, their eruption rate ranges from 130 $m^3\ s^{-1}$ to 2.3×10^7 $m^3\ s^{-1}$ with an average of 1.6×10^6 $m^3\ s^{-1}$. Using the empirically estimated dike lengths, eruption rates range from 2.7×10^2 to 2.4×10^8 $m^3\ s^{-1}$.

Based on a magma viscosity of 1000 Pa s, the transition from a laminar to a turbulent flow regime occurs at a dike width of approximately 20 m. Calculated eruption rates range from 0.03 to 3×10^3 $m^3\ s^{-1}\ m^{-1}$, with an average of 241 $m^3\ s^{-1}\ m^{-1}$. The eruption rates calculated along the total measured dike lengths in eastern Coprates Chasma range from 13 $m^3\ s^{-1}$ to 2.3×10^7 $m^3\ s^{-1}$, with an average of 1.5×10^6 $m^3\ s^{-1}$. Using

the empirically estimated dike lengths, eruption rates range from 27 $m^3\ s^{-1}$to $2.4 \times 10^8\ m^3\ s^{-1}$. Detailed dike eruption rates are given in Table S1 in the supporting information.

6. Discussion

6.1. Dike Dimensions and the Volcanic History of Valles Marineris

In Coprates Chasma walls, 129 linear dike-like features are observed but only a dozen have metamorphic borders and columnar jointing. Due to the limited coverage of high-resolution images (Figure 5e) or lack of spectroscopic data, we cannot exclude that some faults or fractures were mapped as dikes. The composition of one of these dikes (without columnar jointing but with a thick margin) was, however, previously studied and formally identified as a magmatic intrusion [*Flahaut et al.*, 2011], which supports our hypotheses that the linear features are dikes.

Modeling was used to estimate eruption rates for each dike mapped in eastern Coprates Chasma to establish if the dikes were potentially the feeder system to the lavas that form the upper part of the stratigraphy in the region (Figure 2, units C and D). Average eruption rates are on the order of $10^6\ m^3\ s^{-1}$ assuming magma viscosities ranging between 1000 and 10 Pa s. These inferred eruption rates are much higher than terrestrial rates but are in the same order as rates previously reported for Martian fissural eruptions [e.g., *Head et al.*, 2006] (see next section). Typical basaltic eruption rates on Earth are on the order of a few $m^3\ s^{-1}$. For example, the 2014–2015 fissure eruption of Bardarbunga (Iceland) that formed the new Nornahraun lava field had a peak effusion rate between 195 and 280 $m^3\ s^{-1}$ [*Hoskuldsson et al.*, 2015]. The highest historical eruption rate was the 1783–1784 Laki fissure eruption in Iceland, an active fissure of 2.5 km long and several meters wide. The eruption rate was estimated to be 5000 $m^3\ s^{-1}$ with a peak at 8700 $m^3\ s^{-1}$ [*Thordarson and Self*, 1993].

On Mars, *Hauber et al.* [2011] calculated eruption rates of 4.3 $10^2\ m^3\ s^{-1}$ for magmas with high viscosities of 3960 Pa s and 4.6 $10^2\ m^3\ s^{-1}$ for 2530 Pa s for Amazonian lava flows erupted in the Tharsis region near Pavonis Mons. Lava flows east of Jovis Tholus (Tharsis region) were erupted from linear fissures up to 20 km long. Their calculated eruption rates are between 5000 $m^3\ s^{-1}$ and 10,000 $m^3\ s^{-1}$, assuming a magma viscosity of 100 Pa s [*Wilson et al.*, 2009].

The volcanic events investigated in previous studies of the Tharsis region are however recent (<200 Myr), while the fissural eruption investigated in the present study are likely to correspond to older events. Dikes in Coprates Chasma are eroded and often terminate at discrete elevations. Individual dikes are likely to be of different ages but appear to predate the opening of Valles Marineris and be older or synchronous to the late Noachian/ early Hesperian (~3.7 Gyr) plateaus [*Tanaka et al.*, 2014]. The plateau lava deposits must also predate the canyon opening since they are cut open by the chasma. Due to the hotter interior of the planet in the past potentially higher eruption rates could be associated with some Noachian and Hesperian volcanic events. An example is the emplacement of the Hesperian volcanic plains that led to a widespread resurfacing (~22% of the global Martian surface), including the Coprates region [*Tanaka et al.*, 2014]. Fissural eruptions have been studied on the Hesperian plains in the Hellas region [*Head et al.*, 2006]. Using the same equations as in this study, eruption rates of 10^5 and $10^6\ m^3\ s^{-1}$ were calculated for volcanic ridges associated with basalt-flood-like Hesperian plains. These eruption rates are similar to our results (10^2 to $10^7\ m^3\ s^{-1}$ from the smaller to the larger dike), suggesting that eruption rates for Coprates Chasma are consistent with those of pre-Amazonian fissural eruptions.

The plateaus around eastern Coprates Chasma are made of lava flows that can be traced in the upper walls of the trough and have a total average thickness of ~4 km. The surface area where dikes were mapped in the trough is $5 \times 10^{10}\ m^2$. The volume of lava flows in the study area (prior to trough opening) would have been approximately $2 \times 10^5\ km^3$. If we assume that the observed dikes are the sole source of the lava flows located above them, we can estimate the minimum time necessary to form the volcanic layers constituting the upper walls. Such a calculation relies on various assumptions and is therefore subject to uncertainties. Dividing the volume by the lower calculated eruption rates, a duration of 10^3, 10^4, or 10^5 years is implied for a viscosity of 10, 100, and 1000 Pa s, respectively. These calculations suggest that the lava flows could have had a rapid emplacement. This is consistent with the emplacement duration estimated to be less than 1 Myr of the 3 to $5 \times 10^6\ km^3$ of the Siberian trap large igneous province [*Burgess and Bowring*, 2015].

There are however strong uncertainties pertaining to the eruption rates and duration values calculated above, due to necessary oversimplifications:

1. First, it is unlikely that all dikes in the area were mapped. The number of feeder dikes is then underestimated as is the calculated eruption duration.
2. A second and critical point is that dike lengths are difficult to measure and likely underestimated as only short segment is visible in the outcrops and represent an important source of error. Dike emplacement in the region of Coprates Chasma is likely to be similar to dike swarms observed in association with plume tectonic and large igneous provinces. Dikes would propagate laterally and their length could be thousands of kilometer long, as previously reported for giant dike swarms elsewhere on Mars [*Mège and Masson*, 1996; *Wilson and Head*, 2002; *Ernst*, 2014]. If so, all dikes could extend beyond the limit of the study area. Then the calculated eruption rates would be higher. Lengths can also be estimated using an aspect ratio of length/width [*Gudmundsson*, 1984; *Rubin*, 1995]. An aspect ratio equal to 10^3 has also been used for a second set of calculations, resulting in higher eruption rates. The assumed aspect ratio could, however, be influenced by magma viscosity, host rock composition and density, crustal thickness, gradient pressure, etc. [e.g., *Wada*, 1994]. Dikes might also not be active along their entire length during an eruption event. An additional source of error is that it is probable that only a few dikes were active at any one time.
3. There is a possibility that not all dikes propagated vertically and erupted at the surface.
4. Another assumption of our model is a similar magma viscosity for all dikes, whereas viscosities may vary with each individual dike. Dikes in Coprates Chasma have various widths, up to 78 m. *Wada* [1994] concluded from terrestrial observations that magma viscosity has a direct relation with dike width, the most viscous magma forming the wider dikes. Because of internal friction, more viscous magma will increase the force transferred to the host rock producing wider dikes. This in turn makes it more difficult for high-viscosity dikes to travel upward. A change of viscosity could be explained by magma differentiation or by the presence of large crystals or different magma sources. A spectral study by *Flahaut et al.* [2011] for one dike striking 90° revealed a strong signature of olivine suggesting a basaltic composition with large olivine grains. The grain size is also a parameter controlling magma viscosity; the bigger the grains, the higher the viscosity. Further investigations are needed to study the petrology of the dikes. Unfortunately, the spatial resolution of Compact Reconnaissance Imaging Spectrometer for Mars (CRISM) hyperspectral data limits the analyses to the widest dikes, most of which have not yet been imaged with CRISM spectrometer. If (larger) dikes yield higher viscosities, the real eruption rate would be lower than the estimation using a low-viscosity basalt composition. However, the flow velocity is less sensitive to viscosity in the case of turbulent flow regime which is the dominant regime. Then, uncertainty in viscosity is not a major issue.
5. An additional assumption is that the eruption rate would be continuous over the whole eruption duration, which is unlikely. Intermittent magmatic activity have been documented in terrestrial flood basalt provinces like the Deccan Traps, which were emplaced in less than a million year [*Schoene et al.*, 2015] and by a series of individual pulses with durations of several years, with a cumulative active eruption duration spanning only 0.01% of the total formation duration [*Self et al.*, 1997]. Therefore, despite probably under estimating the number of dikes in the crust, our calculations probably give peak eruption rates and might not be representative of the entire eruption duration.

In summary, calculated eruption rates depend on a number of assumptions, with eruption rates of 13 $m^3\ s^{-1}$ to $2.3 \times 10^7\ m^3\ s^{-1}$ for individual dikes and average eruption rates across the entire population of dikes of 1.5×10^6 to $1.6 \times 10^6\ m^3\ s^{-1}$. If at least one dike was active at any given time at the minimum eruption rate, this rate could form the 4 km thick volcanic layers observed in the upper walls of Coprates Chasma within less than a million years. Intermittent eruptions would lengthen this timescale considerably.

6.2. Dike Orientations and Tectonic History of Valles Marineris

Dike emplacement is linked with regional tectonic stress. We interpret the two main sets of dike orientations observed in the east as related to two distinct tectonic episodes, as they propagate perpendicular to the minimum compressive stress in the lithosphere. On Earth, different trends also typically represent different swarms [e.g., *Ernst et al.*, 2001]. We did not observe any clear crosscutting relationships to precisely determine the relative timing of the two dike families, but their maximum elevation in the wall could be an indicator of their relative ages. In eastern Coprates Chasma, dikes oriented 90° appear to be most common. Dikes striking 70° are observed at elevation below ~0 m, whereas those striking 90° appear below 1500 m. If we assume that

the dikes reached the surface when they were emplaced, then the 70° group would be the older set. Linear features striking 70° are present on the plateau, but it is impossible to determine their nature with certainty. If those features are related to the dikes striking 70° then they would suggest that his family is younger. With the impossibility to determine the relative timing of the two families with certainty, we will consider in the following section the dikes striking 70° as older, keeping in mind that it could be the opposite. All the mapped dikes are likely to be older to the late Noachian (3.7 Gyr), the age of the surrounding plateaus as previously estimated by crater counts [e.g., *Tanaka et al.*, 2014; *Loizeau et al.*, 2016]. The 70°-striking dikes appear to have stopped at the level of a paleo-surface of Coprates Chasma (0 m) that predates the topmost lava flows. Later, the emplacement of the second dikes group (striking 90°) under a different stress regime continued to erupt lava flows up to the current plateau elevation (about 3000 m) (Figure 6). These dikes are not detected at elevations $>$1500 m, but we will argue that dike detection may be more difficult due to the less competent and more brittle layers at higher elevations. Due to the greater contrast due to differences in composition, dikes can also be observed more easily in the lower part of the walls. It is also possible that interface between the different layers observed in the walls could prevent dikes to rise into the upper levels. Finally, a different pressure in the magma chamber could also control the dike elevation regardless of the timing. These hypotheses would change our interpretation of their relative age.

In Valles Marineris, small-scale faults trending 70° in Candor Chasma [*Birnie et al.*, 2012] and a set of 65°-striking faults are observed in the walls of Hebes Chasma [*Schmidt*, 2015]. Some of these features are relatively recent as they affect some interior layered deposits, which are dated from the early Hesperian [e.g., *Flahaut et al.*, 2010]. However, the NW wall of Capri Chasma, an ancestral basin located just to the east of our study area, is interpreted as a 70° striking fault and is likely predating the canyon opening [*Yin*, 2012]. The tectonic event responsible for the formation of this fault could be related to the same stress regime that produced the first suite of dikes. Later on, changes in the stress field would have emplaced the second suite of dikes, striking 90°, possibly due to the migration of the stress/volcanic centers within Tharsis and/or the Coprates Rise. Indeed, large-scale radiating dikes are usually observed in association with plume tectonics, and this is typically the case in the Tharsis region [e.g., *Anderson et al.*, 2001]. The long-period duration of Tharsis bulge ($>$3 Gyr) associated with period of quiescence yielded to several distinct magmatic-tectonic centers observed with stratigraphic relations at the surface. Uplift of the Syria Planum province interpreted as a magmatic center may have been associated with a large-scale radial dike swarm due to magma injection in the crust during the late Noachian/early Hesperian and important resurfacing during the early Hesperian [*Mège and Masson*, 1996; *Mege and Ernst*, 2001; *Mège*, 2001; *Ernst et al.*, 2001; *Wilson and Head*, 2002]. Our group of dikes striking 90° in Coprates Chasma is oriented in the approximate direction of Syria Planum early uplift and could be related to this event.

Orientations of tectonic features (grabens, tension cracks, troughs, and wrinkle ridges) were also analyzed by *Anderson et al.* [2001]. Five main tectonic and successive centers were identified. Based only on dike orientation, it remains difficult to connect them to a specific center as only segments are observed. However, dikes in Coprates Chasma were likely formed before the late Hesperian and their orientations (mostly 90°) could indicate that they propagated into the crust from the tectonic center (77°W, 16°S) south-west to Melas Chasma corresponding to stage 2 [*Anderson et al.*, 2001]. However, far away from the magmatic center, local crustal stress will control the dike orientations. Then, dikes can be curved and their orientations in a specific area (e.g., Coprates Chasma) would not give the true direction of their magmatic center.

The opening of Valles Marineris must have occurred after dike emplacement. Based on the observation of the absence of significant uplift on the surrounding Valles Marineris, recent modeling yields to a ratio of 5.7 of vertical subsidence to horizontal extension with normal fault dips greater than 85° in Valles Marineris [*Andrews-Hanna*, 2012a]. It has been proposed that dikes were linked with normal faulting. Hence, dikes could have intruded along fault planes during Valles Marineris formation or, alternatively, faults could have developed along previous dike planes. This would imply a similar orientation between dikes and faults in Valles Marineris. Measured dips in Coprates show that the dikes are indeed steep, often nearly vertical, but there were insufficient data to make definitive conclusions regarding their potential relationship to normal faults.

It is important to note that the orientation of both dike groups as mapped in eastern Coprates Chasma does not match the main orientation of the Valles Marineris canyon/Coprates Chasma walls (110°) which records a third, distinct, tectonic episode. Canyon walls striking 90° and 70°, such as the eastern sets of dikes, are

observed further east in Capri Chasma, Aureum Chaos, and other chaotic terrains. These three different orientations suggest variations in the regional stress field over time and/or location (cf. next section).

Only a few dikes (16) striking subparallel to the Valles Marineris main rift (between 100° and 120°) are present in eastern Coprates Chasma, but they do not appear to represent a distinct group. Dikes striking ~110° were, however, detected in the younger walls of western Coprates Chasma. Fewer dikes are observed in the western walls (18 in total), but they clearly have a different azimuths. Ten of these dikes have orientations between 95° and 130°, and five of them are oriented between 55° to 80°. Clearly, more observations are needed, but a change in dike orientation appears to occur at the approximate location of the Coprates Rise (located at about 58°W longitude), with dikes striking 70° and 90° to the east (Figure 7). This boundary could also be extended to a wider area (still roughly delimited by the Coprates rise) as Candor Chasma's walls (west of the rise) are oriented 110°, contrary to Juventae and Ganges Chamata's southern walls (east of the rise) which are oriented 85° (Figure 7).

The apparent divide between tectonic regimes coincides with a major transition between two distinct crustal lithologies reported by *Flahaut et al.* [2012] and *Quantin et al.* [2012] from the surveys of the walls of Coprates Chasma and the central peaks of surrounding impact craters. These authors suggested the presence of a major discontinuity within Coprates Chasma such as a large-scale tectonic structure or the edge of a basin. Our observations are consistent with two different stress regimes recorded in western and eastern Coprates Chasma, likely in terrains of different age (as the plateaus of western Coprates are mapped as Hesperian), and possibly related to different events. Therefore, the 110° dikes present in western Coprates Chasma could have recorded a third, later, tectonic event related to the main rifting episode. The paucity of dikes oriented 110° in eastern Coprates Chasma and further east could be explained by the presence of a mechanically weak (already heavily fractured) Noachian crust (see next sections).

6.3. Dike Emplacement and Valles Marineris Opening

Dike intrusion has been proposed as a mechanism to form grabens in the region of Tharsis. Grabens are radially oriented around the Tharsis bulge and were interpreted by *Mège and Masson* [1996] and *Wilson and Head* [2002] to be influenced by dike orientations. Dikes striking 90° are oriented in a direction radial to Syria Planum (~2500 km away from the study area) and may be related to an early stage of Tharsis volcanism and graben formations (cf. previous section).

Wyrick et al. [2014] used physical analogue models to try to reproduce grabens after dikes intrusion with little success. Their results suggest that dikes, in the absence of preexisting fault, do not produce sufficient deformation in the crust to initiate graben formation so they favor the faulting origin to form grabens. *Hardy* [2015] pointed out that the absence of crustal deformation in the analogue experiments could be explained by the choice of a nonrealistic thick layer of regolith combined with a basal kinematic discontinuity. Hardy's results are in good agreement with those of *Mastin and Pollard* [1988], who also used an analogue model and found that dike intrusion could induce normal faulting and graben formation.

Dike (or elongated magma chambers) emplacement was also proposed to form larger-scale geologic features such as Valles Marineris troughs, as proposed by *Andrews-Hanna* [2012a, 2012b, 2012c]. In contrast *Schultz and Lin* [2001] proposed that Tharsis load-centered deformation would have induced crustal extension to form Tharsis radial grabens and Valles Marineris through normal faulting.

A scenario has been proposed in which Tharsis loading on the Martian north-south dichotomy boundary caused differential subsidence and crustal extension south of the dichotomy boundary, which would coincide with the present Valles Marineris [*Andrews-Hanna*, 2012a, 2012b, 2012c]. The tensile stress would lead to the propagation of subparallel magmatic intrusions. Lithospheric blocks would be cut, and in the absence of flexural support, block subsidence would initiate trough formation. This late episode of magmatic intrusions (as dikes or large magmatic chambers) would lead to the formation of Valles Marineris. In this scenario, magmatic intrusions would have cut the crust in elongated blocks so we would expect consistent orientation with dike orientation centered on Valles Marineris orientation.

As discussed in the previous section, dikes in eastern Coprates Chasma (mostly striking 90°) have a different orientation to the Chasma itself (110°), which is the main trough connecting the individual troughs and basins of Valles Marineris. Therefore, the link between graben formation and dike intrusion is not straightforward.

However, dikes to the west follow the main trend of Valles Marineris, and some of the eastern Chasmata walls share similar orientations to the eastern sets of dikes (70° and 90°). If the crust of eastern Valles Marineris was already weakened by older 90° and 70° dikes and fractures, a later extensional stress field recorded by the 110° dikes could result in further opening or fault reactivation in the 90° and 70° directions in eastern Valles Marineris rather than the formation of new 110° faults and dikes (e.g., in Ganges, Capri, and Aureum Chasmata). Those chasmata could already have been formed as ancestral basins prior to the main rifting episode. The proposed three-stage tectonic history would explain the global shape of Valles Marineris (110° to the west, with the chaotic terrains further east oriented 90° after 53°W in longitude and 70° between 40°W and 53°W in longitude). The 90° and 70° striking dikes exposed in eastern Coprates Chasma would therefore be interpreted as recording ancient, pre-Valles Marineris events, whereas the dikes in western Coprates Chasma would correspond to younger events and could be synchronous to the first stages of trough formation. Therefore, even though these observations support a link between dike emplacement and the formation of some of Valles Marineris Chasmata (ancestral basins as well as connecting troughs), the timing of faulting versus dike emplacement and opening mechanism remains unclear. We argue that the presence of large volumes of older dikes in the crust could have aided the opening of the troughs by weakening the crust in a specific region (e.g., in eastern Valles Marineris), but the emplacement of dikes is not the sole explanation for the orientation of the canyon, as evidenced in the eastern part of Coprates Chasma.

The formation process of the Martian grabens is also associated with the formation of pit chains, which involves unexplained voids in the crust. Pit chains are linear features consisting of aligned circular troughs. They commonly have kilometer-sized diameter and can be followed along thousands of kilometers. Their origin is still debated, and several hypothesis have been proposed, e.g., collapse of lava tube, collapse of magma chamber, extension fractures, dike intrusion, and interaction with subsurface (see *Wyrick et al.* [2014] for review). North to the eastern part of Coprates Chasma, and west of the Coprates Rise, small-scaled pit chains on the surrounding plateaus are oriented 90°. West to the Coprates Rise, both dikes and pit chains have a similar orientation as Valles Marineris troughs, 110° (cf. section 6.2; Figure 7). Further observations are needed to support a specific hypothesis due to their similar orientation; currently, pit chain formation due to dike intrusion would appear most probable.

7. Proposed Geological History

The oldest unit visible in Valles Marineris' walls is the orthopyroxene-rich basement that is interpreted as pristine crust crystallized from the magma ocean during the pre-Noachian period. This crust has been heavily impacted, fractured, eventually buried, and weathered during the Noachian, the latter resulting in the capping phyllosilicate-rich unit observed in the wall cross section. Dike activity throughout the Noachian and early Hesperian was responsible for the formation of the lava stack observed in the middle and upper walls (also forming extended plains on the plateaus), through fissure eruptions (see section 6.1 [*Mcewen et al.*, 1999] (Figure 8).

The first expression of activity of Tharsis dome during the Noachian period would have produced a set of large-scale radial dikes. The first group is striking 70° dikes and are observed below 0 m in Coprates Chasma walls. These dikes would have produce a large amount of lava flows through fissural eruptions and formed most of the Noachian lava plains (Figure 8a). Possible younger features present on the plateaus around Coprates Chasma could also be related to this dike group. However, it is unclear if these linear features are dikes; thus, the proposed chronology is based on dikes observed in the walls only (and considers the 70° dikes older).

A second radial dikes group striking 90° is observed in Coprates Chasma and is centered in the approximate direction of the early magmatic center identify as Syria Planum. These dikes crosscut the pristine crust, the phyllosilicate layers, and are visible until 1500 m in the upper layers composed of lava flows. These dikes continued to produce lava flows under a different stress field until the early Hesperian period, which is the age of the plateau. Their distribution would be an indicator of the stress rotation from 70° to 90° in the region of eastern Valles Marineris (Figure 8b). Although there is no certainty on the source of this stress field, a migration of volcanic centers within Tharsis or within the Coprates Rise is plausible.

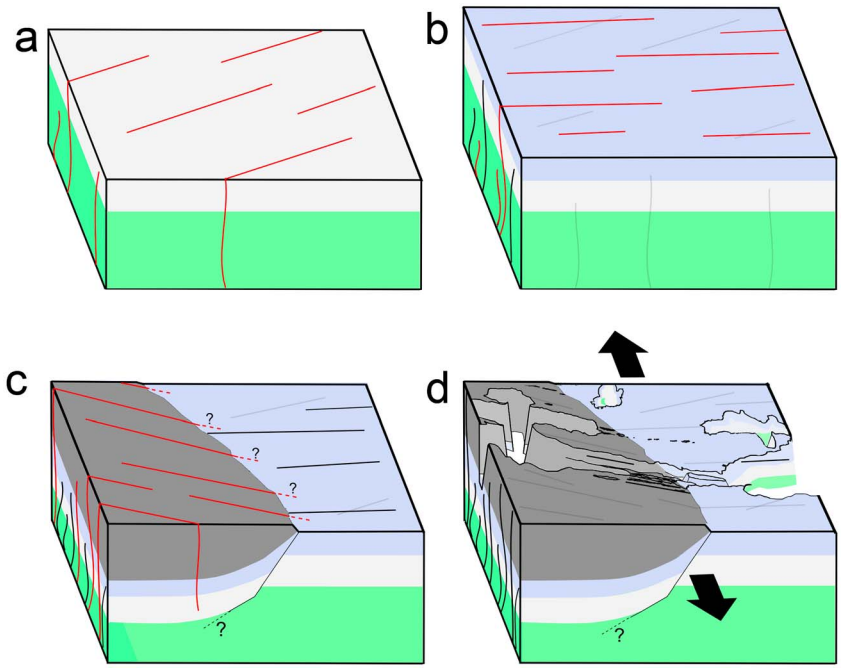

Figure 8. Proposed geologic history. (a) 70° dikes emplacement (red lines) through the Noachian light-toned crust (green basement) and associated lava flows (grey layers) produced by fissural eruptions. Note that Valles Marineris ancestral basins are not represented for simplicity, but they may already exist. (b) 90° dikes emplacement and new associated lava flows (blue layer). (c) Accumulation of volcanic material and formation of the east/west dichotomy, by basin subsidence or early giant impact [see *Quantin et al.*, 2012]. 110° dikes emplacement in the west. (d) North/south extension and opening of Valles Marineris troughs by faulting following dike orientations: 110° in the western part and 90° in the eastern part. Successive dike emplacement could have controlled trough opening. The red, black, and transparent grey are active, nonactive, and buried dikes, respectively.

Observations of dikes striking 90° and 70° only east to the Coprates rise could support the presence of a discontinuity within Valles Marineris as previously suggested by *Flahaut et al.* [2012] and *Quantin et al.* [2012] (Figure 8c). The authors noticed that parts of Valles Marineris were made of distinct material and suggested the presence of a basin filled with Hesperian volcanic products to the west. Tharsis bulge emplacement during the Noachian and Hesperian periods induced stress on the lithosphere. Tharsis bulge emplacement during the Noachian and Hesperian periods induced stress on the lithosphere and could have induced subsidence and faulting of the lithosphere forming an east-west discontinuity around the location of the Coprates rise. Support for this interpretation is given by features with different orientation: (1) in the east, 90° Juventae and Ganges Chasmata southern walls, 90° eastern Coprates Chasma southern wall and small-scale pit chains in Ophir Planum, and 70° Capri and Eos Chasmata walls and (2) in the west, 110° Candor Chasma, Coprates Catenae walls; 110° pit chains north to Thaumasia Planum; and 110° pit chains north to Ophir Chasma.

The final major tectonic stage would have been the opening of the canyon with a 110° orientation during the Hesperian or later [e.g., *Quantin et al.*, 2004] (Figure 8d). The opening would follow the direction of newly Tharsis-induced dikes in western Valles Marineris and have completed the linkage of ancestral basins. Capri Chasma and Ganges Chasma in eastern Valles Marineris could represent such basins formed during previous tectonic stages as the fault delimitating their walls strike mostly 90° and 65° (Capri NW wall). The presence of preexisting faults with these orientations in eastern Valles Marineris, which is made of an older, heavily fractured basement could have prevented the formation of 110° faults and dikes if existing fractures and faults were reused. This hypothesis would explain the current shape of Valles Marineris, as Coprates Chasma graben is oriented 110° in the west and appears to be turning at Capri Chasma, which is roughly oriented at 65°. The formation of chaotic terrains further east also seems controlled by 65° oriented faults among others. Further evidence for volcanism inside the canyon after its formation is localized and includes volcanic cones [e.g., *Brož et al.*, 2015; *Hauber et al.*, 2015] aligned 110° and 70°, which emplacement could have reused existing fractures or faults.

8. Conclusion

A comprehensive survey of the eastern part of Coprates Chasma recorded more than a hundred dikes. The dikes formed in two, possibly unrelated, tectonic events: the first set (70°-striking dikes) is observed up to elevations of 0 m and the second set (90°-striking dikes) is observed up to elevations +1500 m. Their precise chronology is unclear; possible dikes on the plateau (+3500 m) are oriented ~70° and could be related to the 70°-striking dike family, implying that 70°-striking dikes are more recent,. However, the highest group observed in the walls (90°-striking dikes) could be the most recent as they crosscut younger geological units. Dike families in eastern Coprates Chasma do not match the main Valles Marineris orientation (~110°). However, small-scaled pit chains and elongated troughs north of the eastern part of Coprates Chasma, the south walls of Juventae and Ganges chasmata, are also oriented 85° to 90° comparable to one dike generation in Coprates Chasma walls. The mean dike orientation seems to change in the western part of Coprates Chasma, matching orientation of troughs and pit chains (110°) that occur to the west to the approximate location of the Coprates rise and of the crustal discontinuity suggested by *Flahaut et al.* [2012] and *Quantin et al.* [2012]. We propose that these dikes that are observed in younger, Hesperian terrains correspond to a third, later, tectonic event recording the formation of Valles Marineris connecting troughs. Although there are clear correlations between the dikes and some chasmata's orientations, in accordance with *Andrews-Hanna* [2012c] model, it remains unclear if the dike emplacement could have induced the faulting or if magmatic intrusions are the results of passive rifting. In addition, some dike and chasma orientations do not match (e.g., eastern Coprates Chasma), implying a complex tectonic history.

Average eruption rates are on the order of 10^6 m^3 s^{-1} assuming magma viscosities between 1000 and 10 Pa s, respectively, and suggest that dikes could have fed the Noachian and Hesperian lava flows observed at the top of Coprates Chasma, forming the plateaus in less than a million years and potentially in as little as a few hundred years in the case of theoritical continuous and simultaneous eruptions. Further work include petrologic characterization of the dikes which could help in improving these estimates.

Acknowledgments

The authors would like to thank the mission instrument teams, especially the CTX and HiRISE teams for the availability of the data. The authors would like to thank Alfred McEwen personally for his assistance in requesting additional HiRISE imagery. We are also grateful to Pierre Thomas, Damien Loizeau, and the e-Mars team (http://e-mars.geologie-lyon.fr/) for constructive discussions in the early stages of preparation of the manuscript. C. Brustel is funded by the Netherlands Organisation for Scientific Research (NWO) User's support program. J. Flahaut was supported by a CNES postdoctoral fellowship at the time of the project. G.R. Davies is partly funded by ERC Synergy grant 319209; "Nexus 1492." Supporting information can be asked to the author at the address c.p.a.brustel@vu.nl. Cathy Quantin-Nataf is supported by European Research Council through the FP7/2007-2013/ERC grant agreement 280168. Finally, the authors would like to thank David Baratoux, Richard Ernst, and an anonymous reviewer for their very helpful comments and availability during the reviews stages.

References

Anderson, R. C., J. M. Dohm, M. P. Golombek, A. F. C. Haldemann, B. J. Franklin, K. L. Tanaka, J. Lias, and B. Peer (2001), Primary centers and secondary concentrations of tectonic activity through time in the western hemisphere of Mars, *J. Geophys. Res.*, *106*(E9), 20,563, doi:10.1029/2000JE001278.

Andrews-Hanna, J. C. (2012a), The formation of Valles Marineris: 1. Tectonic architecture and the relative roles of extension and subsidence, *J. Geophys. Res.*, *117*, E03006, doi:10.1029/2011JE003953.

Andrews-Hanna, J. C. (2012b), The formation of Valles Marineris: 2. Stress focusing along the buried dichotomy boundary, *J. Geophys. Res.*, *117*, E04009, doi:10.1029/2011JE003954.

Andrews-Hanna, J. C. (2012c), The formation of Valles Marineris: 3. Trough formation through super-isostasy, stress, sedimentation, and subsidence, *J. Geophys. Res.*, *117*, E06002, doi:10.1029/2012JE004059.

Baker, V. R., M. H. Carr, V. C. Gulick, R. C. Williams, and M. S. Marley (1992), Channels and Valley networks, in *Mars*, pp. 493–522, Univ. of Ariz. Press, Space Sci. Ser.

Baragar, W. R. A., R. E. Ernst, L. Hulbert, and T. Peterson (1996), Longitudinal Petrochemical Variation in the Mackenzie Dyke Swarm, Northwestern Canadian Shield, *J. Petrol.*, *37*(2), 317–359, doi:10.1093/petrology/37.2.317.

Birnie, C., F. Fueten, R. Stesky, and E. Hauber (2012), Underlying structural control of small-scale faults and fractures in West Candor Chasma, Mars, *J. Geophys. Res.*, *117*, E11001, doi:10.1029/2012JE004144.

Broxton, M., and L. Edwards (2008), The Ames Stereo Pipeline: Automated 3D surface reconstruction from orbital imagery, *Lunar Planet. Sci. Conf. (Vol. 39)*, *1461*, 2419.

Brož, P., O. Čadek, E. Hauber, and A. P. Rossi (2015), Scoria cones on Mars: Detailed investigation of morphometry based on high-resolution digital elevation models, *J. Geophys. Res. Planets*, *120*, 1512–1527, doi:10.1002/2015JE004873.

Burgess, S. D., and S. A. Bowring (2015), High-precision geochronology confirms voluminous magmatism before, during, and after Earth's most severe extinction, *Sci. Adv.*, *1*(7), e1500470–e1500470, doi:10.1126/sciadv.1500470.

Carr, M. H. (1974), Tectonism and volcanism of the Tharsis region of Mars, *J. Geophys. Res.*, *79*(26), 3943–3949, doi:10.1029/JB079i026p03943.

Cattermole, P. (1987), Sequence, rheological properties, and effusion rates of volcanic flows at Alba Patera, Mars, *J. Geophys. Res.*, *92*(B4), E553–E560, doi:10.1029/JB092iB04p0E553.

Chevrel, M. O. (2013), Rheology of Martian lava flows: An experimental approach.

Croft, S. (1989), Spelunking on Mars: The carbonate-tectonic hypothesis for the origin of Valles Marineris, *Tecton. Featur. Mars*.

Ernst, R. E. (2014), *Large Igneous Provinces*, pp. 179–213, Cambridge Univ. Press, Cambridge.

Ernst, R. E., and K. Bell (1992), Petrology of the great abitibi dyke, superior province, Canada, *J. Petrol.*, *33*(2), 423–469, doi:10.1093/petrology/33.2.423.

Ernst, R. E., E. B. Grosfils, and D. Mège (2001), GIANT DIKE SWARMS: Earth, Venus, and Mars, *Annu. Rev. Earth Planet. Sci.*, *29*(2001), 489–534, doi:10.1146/annurev.earth.29.1.489.

Flahaut, J., C. Quantin, P. Allemand, and P. Thomas (2010), Morphology and geology of the ILD in Capri/Eos Chasma (Mars) from visible and infrared data, *Icarus*, *207*(1), 175–185, doi:10.1016/j.icarus.2009.11.019.

Flahaut, J., J. F. Mustard, C. Quantin, H. Clenet, P. Allemand, and P. Thomas (2011), Dikes of distinct composition intruded into Noachian-aged crust exposed in the walls of Valles Marineris, *Geophys. Res. Lett.*, *38*, L15202, doi:10.1029/2011GL048109.

Flahaut, J., C. Quantin, H. Clenet, P. Allemand, J. F. Mustard, and P. Thomas (2012), Pristine Noachian crust and key geologic transitions in the lower walls of Valles Marineris: Insights into early igneous processes on Mars, *Icarus*, *221*(1), 420–435, doi:10.1016/j.icarus.2011.12.027.

Fueten, F., R. Stesky, P. Mackinnon, E. Hauber, T. Zegers, K. Gwinner, F. Scholten, and G. Neukum (2008), Stratigraphy and structure of interior layered deposits in west Candor Chasma, Mars, from High Resolution Stereo Camera (HRSC) stereo imagery and derived elevations, *J. Geophys. Res.*, *113*, E10008, doi:10.1029/2007JE003053.

Fueten, F., J. Flahaut, L. Le Deit, R. Stesky, E. Hauber, and K. Gwinner (2011), Interior layered deposits within a perched basin, southern Coprates Chasma, Mars: Evidence for their formation, alteration, and erosion, *J. Geophys. Res.*, *116*, E02003, doi:10.1029/2010JE003695.

Gudmundsson, A. (1984), Tectonic aspects of dykes in northwestern Iceland, *Jökull*, *34*, 81–96.

Hardy, S. (2015), Does shallow dike intrusion and widening remain a possible mechanism for graben formation on Mars?, *Geology*, *44*(2), 107–110, doi:10.1130/G37285.1.

Hare, T. M., S. W. Akins, R. M. Sucharski, M. S. Bailen, and J. A. Anderson (2013), Map projection web service for PDS images, *44th Lunar Planet. Sci. Conf.*, *86001*, abstract 2068.

Hauber, E., P. Brož, F. Jagert, P. Jodowski, and T. Platz (2011), Very recent and wide-spread basaltic volcanism on Mars, *Geophys. Res. Lett.*, *38*, L10201, doi:10.1029/2011GL047310.

Hauber, E., P. Brož, A. P. Rossi, and G. Michael (2015), A field of small pitted cones on the floor of Coprates Chasma mars: Volcanism inside Valles Marineris? E., *46th Lunar Planet. Sci. Conf.*, 3–4.

Head, J. W., L. Wilson, J. Dickson, and G. Neukum (2006), The Huygens-Hellas giant dike system on Mars: Implications for late Noachian-early Hesperian volcanic resurfacing and climatic evolution, *Geology*, *34*(4), 285–288, doi:10.1130/G22163.1.

Hiesinger, H., J. W. Head III, and G. Neukum (2007), Young lava flows on the eastern flank of Ascraeus Mons: Rheological properties derived from High Resolution Stereo Camera (HRSC) images and Mars Orbiter Laser Altimeter (MOLA) data, *J. Geophys. Res.*, *112*, E05011, doi:10.1029/2006JE002717.

Hoskuldsson, A., I. Jónsdóttir, M. S. Riishus, G. B. M. Pedersen, M. T. Gudmundsson, T. Thordarson, and V. Drouin (2015), Magma discharge and lava flow field growth in the Nornahraun/Bardarbunga eruption Iceland, *Geophys. Res. Abstr. EGU Gen. Assem.*, *17*, 2015–12755.

Johnson, C. L., and R. J. Phillips (2005), Evolution of the Tharsis region of Mars: Insights from magnetic field observations, *Earth Planet. Sci. Lett.*, *230*(3–4), 241–254, doi:10.1016/j.epsl.2004.10.038.

Loizeau, D., J. Carter, C. Millot, J. Flahaut, C. Quantin, P. Thollot, and L. Lozac'h (2016), Widespread aqueous surface weathering south of Coprates Chasma, Mars., *47th LPSC*, 2014–2015, doi:10.1038/ngeo2474.

Longhi, J. (1990), Magmatic processes on Mars: Insights from SNC meteorites, *Lunar Planet. Sci. Conf.*, *21*, 716.

Lucchitta, B. K., N. K. Isbell, and A. Howington-Kraus (1994), Topography of Valles Marineris: Implications for erosional and structural history, *J. Geophys. Res.*, *99*(E2), 3783–3798, doi:10.1029/93JE03095.

Malin, M. C., et al. (2007), Context Camera investigation on board the Mars Reconnaissance Orbiter, *J. Geophys. Res.*, *112*, E05S04, doi:10.1029/2006JE002808.

Mastin, L. G., and D. D. Pollard (1988), Surface deformation and shallow dike intrusion processes at Inyo craters, Long Valley, California, *J. Geophys. Res.*, *93*(B11), 13221–13235, doi:10.1029/JB093iB11p13221.

McEwen, A. S., M. C. Malin, M. H. Carr, and W. K. Hartmann (1999), Voluminous volcanism on early Mars revealed in Valles Marineris, *Nature*, *397*(8003), 584–586.

McEwen, A. S., et al. (2007), Mars Reconnaissance Orbiter's High Resolution Imaging Science Experiment (HiRISE), *J. Geophys. Res.*, *112*, E05S02, doi:10.1029/2005JE002605.

Mège, D. (2001), Uniformitarian plume tectonics: The post-Archean Earth and Mars, *Geol. Soc. Am. Spec. Pap.*, *352*, 141–164, doi:10.1130/0-8137-2352-3.141.

Mege, D., and R. E. Ernst (2001), Contractional effects of mantle plumes on Earth, Mars, and Venus, *Geol. Soc. Am. Spec. Pap.*, *352*, 103–140, doi:10.1130/0-8137-2352-3.103.

Mège, D., and P. Masson (1996), A plume tectonics model for the Tharsis province, Mars, *Planet. Space Sci.*, *44*(I), 1499–1546, doi:10.1016/S0032-0633(96)00113-4.

Moore, H. J., D. W. G. Arthur, and G. G. Schaber (1978), Yield strengths of flows on the Earth, Mars, and Moon, *Lunar Planet. Sci. Conf.*, *3*(A79–39253), 16–91.

Moratto, S. Z. M., M. J. Broxton, R. A. Beyer, M. Lundy, and K. Husmann (2010), Ames Stereo Pipeline, NASA 's Open Source Automated Stereogrammetry, *41st Lunar Planet. Sci. Conf.*, 1–2.

Quantin, C., P. Allemand, N. Mangold, and C. Delacourt (2004), Ages of Valles Marineris (Mars) landslides and implications for canyon history, *Icarus*, *172*(2), 555–572, doi:10.1016/j.icarus.2004.06.013.

Quantin, C., J. Flahaut, H. Clenet, P. Allemand, and P. Thomas (2012), Composition and structures of the subsurface in the vicinity of Valles Marineris as revealed by central uplifts of impact craters, *Icarus*, *221*(1), 436–452, doi:10.1016/j.icarus.2012.07.031.

Rubin, A. M. (1995), Propagation of magma-filled cracks, *Annu. Rev. Earth Planet. Sci.*, *23*, 287–336, doi:10.1146/annurev.ea.23.050195.001443.

Schmidt, G. (2015), *Geology of Hebes Chasma*, Valles Marineris, Mars.

Schoene, B., K. M. Samperton, M. P. Eddy, G. Keller, T. Adatte, S. A. Bowring, S. F. R. Khadri, and B. Gertsch (2015), U-Pb geochronology of the Deccan Traps and relation to the end-Cretaceous mass extinction, *Science*, *347*(6218), 182–184, doi:10.1126/science.aaa0118.

Schultz, R. A. (1998), Multiple-process origin of Valles Marineris basins and troughs, Mars, *Planet. Space Sci.*, *46*(6–7), 827–834, doi:10.1016/S0032-0633(98)00030-0.

Schultz, R. A., and J. Lin (2001), Three-dimensional normal faulting models of the Valles Marineris, Mars, and geodynamic implications, *J. Geophys. Res.*, *106*(B8), 16549–16566, doi:10.1029/2001JB000378.

Self, S., T. Thordarson, and L. Keszthelyi (1997), Emplacement of continental flood basalt lava flows, *Large Igneous Prov. Cont. Ocean. Planet. Flood Volcanism*, *2*, 381–410, doi:10.1029/GM100.

Sharp, R. P. (1973), Mars: Troughed terrain, *J. Geophys. Res.*, *78*(20), 4063, doi:10.1029/JB078i020p04063.

Smith, D. E., et al. (2001), Mars Orbiter Laser Altimeter: Experiment summary after the first year of global mapping of Mars, *J. Geophys. Res.*, *106*(E10), 23689–23722, doi:10.1029/2000JE001364.

Tanaka, K. L., and M. P. Golombek (1989), Martian tension fractures and the formation of grabens and collapse features at Valles Marineris, *Proc. 19th Lunar Planet. Sci. Conf.*, 383–396, doi:10.1017/CBO9781107415324.004.

Tanaka, K. L., S. J. Robbins, C. M. Fortezzo, J. A. Skinner, and T. M. Hare (2014), The digital global geologic map of Mars: Chronostratigraphic ages, topographic and crater morphologic characteristics, and updated resurfacing history, *Planet. Space Sci.*, *95*, 11–24, doi:10.1016/j.pss.2013.03.006.

Thordarson, T., and S. Self (1993), The Laki (Skaftdr fires) and Grimsv6tn eruptions in 1783–1785, *Bull. Volcanol.*, *55*, 233–263.

Wada, Y. (1994), On the relationship between dike width and magma viscosity, *J. Geophys. Res.*, *99*(B9), 17,743–17,755, ST–On the Relationship between Dike.

Wilson, L., and J. W. Head (1981), Ascent and eruption of basaltic magma on the Earth and Moon, *J. Geophys. Res.*, *86*(B4), 2971, doi:10.1029/JB086iB04p02971.

Wilson, L., and J. W. Head (2001), Lava fountains from the 1999 Tvashtar Catena fissure eruption on Io: Implications for dike emplacement mechanisms, eruption rates, and crustal structure, *J. Geophys. Res.*, *106*(E12), 32997, doi:10.1029/2000JE001323.

Wilson, L., and J. W. Head (2002), Tharsis-radial graben systems as the surface manifestation of plume-related dike intrusion complexes: Models and implications, *J. Geophys. Res.*, *107*(E8), 5057, doi:10.1029/2001JE001593.

Wilson, L., P. J. Mouginis-Mark, S. Tyson, J. Mackown, and H. Garbeil (2009), Fissure eruptions in Tharsis, Mars: Implications for eruption conditions and magma sources, *J. Volcanol. Geotherm. Res.*, *185*(1–2), 28–46, doi:10.1016/j.jvolgeores.2009.03.006.

Wise, D. U., M. P. Golombek, and G. E. McGill (1979), Tharsis province of Mars: Geologic sequence, geometry, and a deformation mechanism, *Icarus*, *38*(3), 456–472, doi:10.1016/0019-1035(79)90200-8.

Wyrick, D. Y., A. P. Morris, M. K. Todt, and M. J. Watson-Morris (2014), Physical analogue modelling of Martian dyke-induced deformation, *Volcanism Tectonism Across Inn. Sol. Syst. Geol. Soc. London, Spec. Publ.*, *401*, 395–403, doi:10.1144/SP401.15.

Yin, A. (2012), Structural analysis of the Valles Marineris fault zone: Possible evidence for large-scale strike-slip faulting on Mars, *Lithosphere*, *4*(4), 286–330, doi:10.1130/L192.1.

Zimbelman, J. R. (1985), Estimates of rheologic properties for flows on the Martian volcano Ascraeus Mons, *J. Geophys. Res.*, *90*(S01), 157, doi:10.1029/JB090iS01p00157.